

Mechanics-Based Control of Underactuated 3D Robotic Walking: Dynamic Gait Generation Under Torque Constraints

Matthew J. Powell and Aaron D. Ames

Abstract—This paper presents a novel method of stabilizing hybrid models of torque-constrained, underactuated walking robots – without using nonlinear gait optimization – by leveraging properties of the mechanics of the robot. At its core, the controller stabilizes the transfer of angular momentum from one leg to the next through continuous-time control coupled with hybrid system models that capture impacts that occur at foot strike. In particular, conservation of angular momentum at impact allows for computation of the exact transfer of momentum as a function of the robot’s step length and vertical center of mass velocity just prior to foot impact. This motivates the construction of continuous-time reference trajectories for the robot’s step length and vertical center of mass with endpoints corresponding to a desired transfer of angular momentum. Stabilization to these trajectories results in stable walking, as indicated by numeric Poincaré analysis. The controller is implemented in simulation of a five-link, underactuated 3D robot via Model Predictive Control which provides a means of achieving walking under non-trivial actuation limits.

I. INTRODUCTION

The five-link, underactuated robot biped considered in this paper is characterized by a lack of feet: the robot’s lower leg contacts the ground at a single, unactuated point. Achieving stable walking via control of this system is not just a matter of placing one foot in front of the other; the passive interface between the robot and the ground corresponds to two modes of the system that are uncontrollable in continuous-time and impacts between the robot and the ground impart discrete changes in the robot’s velocity. To date, successful methods of stabilizing this class of walking robots have leveraged mathematical properties of robot models to construct nonlinear optimization problems which solve for stable gaits, see for example [2], [6], [16], [23]. This paper presents a novel approach built upon the mechanics of underactuated robotic walking – augmented with nonlinear control design – to produce controllers without use of offline gait optimization.

The proposed mechanics-based control approach focuses on the stabilization of the evolution of the angular momentum about the robot’s support pivot; this quantity accounts for two of the eight degrees of freedom in the 3D underactuated biped considered. However, the rate of change of angular momentum about the support pivot in underactuated walking is influenced only by gravity. The robot’s actuators can work to manipulate the effect of gravity by modifying the robot’s shape and thereby changing the moment-arm by which gravity operates; but the actuators cannot affect the instantaneous

rate of change of angular momentum (in mathematical terms, the angular momentum about the support pivot is one of the zero dynamics coordinates [23]). To keep the angular momentum from blowing up and causing instability, the proposed control approach operates on the transfer of angular momentum associated with stepping.

The conjecture of this work is that part of the fundamental mechanics of stable underactuated walking is the stabilization of the transfer of angular momentum from one leg to the next. Indeed, one mathematical criterion for stable walking via Hybrid Zero Dynamics is that the fixed point of the Poincaré map for the HZD of a given continuous-time controller must be exponentially stable (see Theorem 3 of [23]). This statement, together with the fact that part of the zero dynamics of underactuated walking is the rate of change of angular momentum about the support pivot, suggests that walking might be stabilized through regulation of angular momentum in discrete-time. Rather than first constructing parameterized continuous-time controllers and then using optimization to solve for parameters that result in a stable hybrid zero dynamics – as is done in the HZD-based approaches – the present method seeks to directly stabilize the discrete-time angular momentum by manipulating the kinematics of the robot at impact. In particular, the transfer of angular momentum from one leg to the next can be computed exactly as a function of the robot’s swing leg position and center of mass velocity. This motivates the design of continuous-time desired trajectories for the swing leg and the vertical center of mass which have endpoints corresponding to a desired transfer of momentum.

The specific choice of desired transfer of angular momentum is obtained through use of the Linear Inverted Pendulum (LIP) model [10], a widely used concept in the contemporary robotic walking community. One of the most successful walking controllers that employs the LIP, the Capture Point [18] method uses the phase space of the LIP to suggest stepping strategies which ensure that the robot is capable of taking another step or stopping. As the LIP is traditionally used in impact-less robot models, the current paper makes modifications to the typical LIP in order to use it for the nonlinear, hybrid model of interest. In particular, the LIP is used in the present paper to predict the evolution of the angular momentum about the support pivot – instead of predicting the center of mass velocity. Consequently, conservation of angular momentum properties of the nonlinear impact model can be used to incorporate (exact) discrete-time effects in this angular momentum variant of the LIP, and thus capture the hybrid nature of the model of interest.

This research is supported by NSF award 1562236.

Matthew J. Powell and Aaron D. Ames are with the Department of Mechanical Engineering, Georgia Institute of Technology, Atlanta, GA 30308. {mpowell135, ames}@gatech.edu

The proposed controller is implemented on the full robot dynamics via Model Predictive Control [14], [17], [21], which provides a method of stabilizing underactuated walking in the presence of non-trivial torque bounds. This is similar to several existing methods to stabilizing walking under torque bounds in the literature, such as Differential Dynamic Programming [22] and ZMP Quadratic Programming [12].

It is important to note that the mechanics of walking has played a large role in the development of many robot walking control strategies to-date, particularly in the control of footed robots; in addition to the LIP, the Spring-Loaded Inverted Pendulum [4] and the Zero Moment Point [9] are inherently mechanics-based control concepts. Alternative methods of angular momentum-based control of walking have been considered before in [11], [13], and a recent extension of HZD includes angular momentum considerations in the offline optimization of nonholonomic constraints for walking [5]. To the author’s knowledge, however, the present method is one of the first (in addition to [19]) to drive the underactuated robot of interest into an asymptotically stable periodic orbit, as indicated by numeric Poincaré analysis [8], without offline optimization. This points to the possibility of real-time gait generation utilizing the nonlinear and hybrid aspects of the underactuated robot mechanics.

II. UNDERACTUATED ROBOT MODEL

The robot, shown in Fig. 1, is modeled as a rigid-body tree comprised of five links and six actuators, as in [6]. The base of the tree is located at the bottom of the support leg; it is assumed that sufficient friction prevents the support leg from sliding on the ground and from rotating about the axis perpendicular to the ground (the \hat{z} axis). Two rotations, $\mathbf{q}_u = (q_1, q_2)^T$, are used to describe the rotation of the support calf about the world \hat{x} and \hat{y} axes; and six relative (intrinsic) rotations, $\mathbf{q}_a = (q_3, q_4, \dots, q_8)^T$, are used to describe the actuated joint angles, which are acted upon by joint torques $\mathbf{u} = (u_1, u_2, \dots, u_6)^T$, in order. The collection of unactuated and actuated angles will often be referred to as a single, “joint angle” vector $\mathbf{q} = (q_1, q_2, \dots, q_8)^T$. This section discusses properties of the robot model that will be used in the construction of the proposed mechanics-based control approach to walking.

A. Angular Momentum

The angular momentum about the support pivot in the underactuated robot biped is a vector quantity given by $\mathbf{L} = \mathbf{r}_c \times m\mathbf{v}_c + \mathbf{H}$ where $\mathbf{r}_c = (x_c, y_c, z_c)^T$ and $\mathbf{v}_c = (\dot{x}_c, \dot{y}_c, \dot{z}_c)^T$ are the center of mass position and velocity relative to the support foot, m is the mass of the robot and \mathbf{H} is the centroidal angular momentum. As mentioned, the rotation about the vertical, \hat{z} , axis is constrained (through sufficient friction) to be constant. However, the robot is free to pivot about the forward, \hat{x} , and lateral, \hat{y} , axes corresponding to respective components of angular momentum L_x and L_y about the support pivot

$$\begin{pmatrix} L_x \\ L_y \end{pmatrix} = \begin{pmatrix} my_c \dot{z}_c - mz_c \dot{y}_c + H_x \\ mz_c \dot{x}_c - mx_c \dot{z}_c + H_y \end{pmatrix}. \quad (1)$$

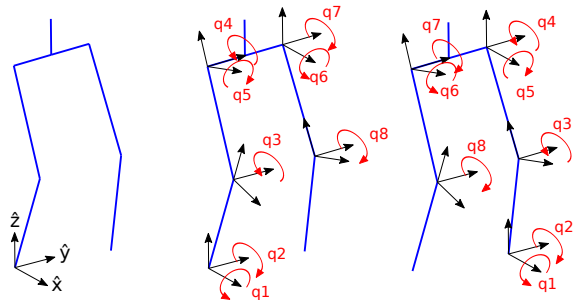


Fig. 1. (Left) the base of the kinematic chain is currently located at the end of the right leg. (Middle) shows the coordinates used in the underactuated biped robot when the right leg is the support leg and (right) shows coordinates when the left leg is the support leg .

The instantaneous rate of change of angular momentum about the support pivot point is a passive quantity

$$\begin{pmatrix} \dot{L}_x \\ \dot{L}_y \end{pmatrix} = \begin{pmatrix} -mgy_c \\ mgx_c \end{pmatrix}, \quad (2)$$

where g is the constant acceleration due to gravity. This fact plays a large role in the proposed mechanics-based controller.

B. Equations of motion

As in [7], the equations of motion for the actuated coordinates are obtained through the Euler-Lagrange method. Letting T denote the kinetic energy and V denote the potential energy in the system, the Euler-Lagrange equations take the form

$$\frac{d}{dt} \left(\frac{\partial T}{\partial \dot{\mathbf{q}}_a} \right) - \frac{\partial (T - V)}{\partial \mathbf{q}_a} = \mathbf{u}. \quad (3)$$

These equations together with the rate of change of angular momentum in the lateral and forward directions (2) constitute the dynamics model. Letting $\mathbf{x} = (\mathbf{q}, \dot{\mathbf{q}})$, the equations of motion can be written $\dot{\mathbf{x}} = f(\mathbf{x}) + g(\mathbf{x})\mathbf{u}$.

C. Impact Model and Coordinate Relabeling

In the model considered, impacts between the robot and the ground cause discrete changes in the robot’s linear momentum and joint velocities, resulting in a hybrid system model. This paper employs the impact model described in [7], wherein impacts are assumed to be perfectly inelastic and to occur over an infinitesimal time. Quantities just-prior to impact are referred to as “pre-impact” and denoted \square^- , post-impact quantities are denoted \square^+ . The discrete change in joint-angle velocities due to impact takes the form

$$\dot{\mathbf{q}}^+ = \Delta(\mathbf{q}^-)\dot{\mathbf{q}}^-, \quad (4)$$

see [7] for a definition of $\Delta(\mathbf{q}^-)$. A key property of this impact model is that the forward and lateral components of angular momentum about the point of impact are conserved

$$\begin{pmatrix} L_x^+ \\ L_y^+ \end{pmatrix} = \begin{pmatrix} L_x^- \\ L_y^- \end{pmatrix}. \quad (5)$$

This fact is exploited in the proposed mechanics-based walking controller. Finally, as the base of the kinematic chain is located at the support foot, a relabeling procedure is used to “re-base” the coordinates when the robot takes a step [7].

III. UNDERACTUATED WALKING MECHANICS

The robot model of interest is a nonlinear hybrid system. Producing walking controllers for this type of system has historically required use of nonlinear optimization; however, the present paper leverages properties of the mechanics of the model to construct walking gaits without the use of (offline) optimization. In this section, it is shown that the Linear Inverted Pendulum can be used to characterize the evolution of the angular momentum about the support pivot in the (nonlinear) underactuated walking model. Additionally, conservation of angular momentum is used to derive an exact expression for the transfer of angular momentum from one leg to the next. These properties are used in the construction of the proposed control method discussed later in the paper.

A. Continuous-Time Momentum Characterization

The LIP is traditionally used to estimate the evolution of the robot's forward COM velocity; however, the current paper presents a variation of the LIP which instead predicts the evolution of the angular momentum about the support pivot. The following derivation is for the forward momentum, but the equations are nearly identical for the lateral momentum. Recall that in the underactuated robot model, the rate of change of angular momentum (2) is a nonlinear expression

$$mz_c\ddot{x}_c - mx_c\ddot{z}_c + \dot{H}_y = mgx_c. \quad (6)$$

The Linear Inverted Pendulum model can be obtained from (6) by setting the vertical height of the center of mass to a constant $z_c \equiv z_0$, thus $\ddot{z}_c \equiv 0$, and setting $\dot{H}_y = 0$

$$mz_0\ddot{x}_c = mgx_c. \quad (7)$$

Let $x_L(t)$ denote the solution of the LIP dynamics (7)

$$x_L(t) = c_1 e^{\lambda t} + c_2 e^{-\lambda t}, \quad (8)$$

where $\lambda = \sqrt{\frac{g}{z_0}}$ and c_1 and c_2 are functions of the initial condition. In traditional usage of the LIP model, c_1 and c_2 are functions of the initial position $x_c(0)$ and velocity $\dot{x}_c(0)$; however, in the present paper, c_1 and c_2 are designed using the initial center of mass position and the angular momentum

$$c_2 = \frac{1}{2}x_c - \frac{L_y}{2m\lambda z_0}, \quad (9)$$

$$c_1 = x_c - c_2, \quad (10)$$

through the relationship between velocity and angular momentum $L_y = mz_0\dot{x}_c$; this variation on the LIP plays an important role in the construction of the proposed walking controller. The derivative of (8) provides an estimate of the evolution of the angular momentum in the system

$$L_y(t) = mz_0\lambda (c_1 e^{\lambda t} - c_2 e^{-\lambda t}). \quad (11)$$

The ‘‘phase space’’ for this system is shown in Fig. 2. Note that the origin is a saddle and the asymptotes $L_y = \pm x_c \sqrt{gz_0}$ partition the space into four domains. As the flow in the top domain corresponds to forward motion in the x direction, the goal will be to ensure that the system returns to the top domain after every step through proper regulation of momentum transfer due to stepping.

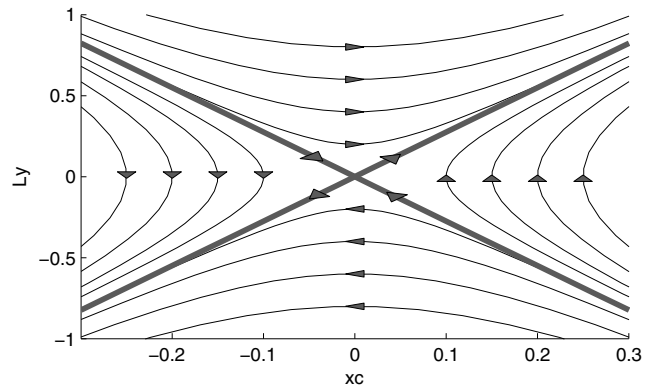


Fig. 2. A variant of the Linear Inverted Pendulum phase space, for $z_0 = 0.7\text{m}$ and $m = 1\text{kg}$, is used to characterize the evolution of the forward angular momentum and the relative horizontal center of mass in underactuated walking. The goal of the mechanics-based control implementation is to ensure that the transfer of momentum due to stepping returns the angular momentum and COM to the top (forward walking) quadrant.

B. Momentum Transfer

Let $\mathbf{r}_s = (x_s, y_s, z_s)^T$ denote the vector from the support pivot to the swing foot. When the swing foot impacts the ground, support of the robot transfers from the current support pivot to the point of impact. The corresponding transfer of angular momentum about the current pivot, $\mathbf{L}[k]$, $k \in \mathbb{N}_0$, to angular momentum about the next, $\mathbf{L}[k+1]$, can be obtained through direct computation

$$\mathbf{L}[k+1] = \mathbf{L}[k] - \mathbf{r}_s[k] \times m\mathbf{v}_c[k]. \quad (12)$$

Furthermore, as angular momentum is conserved about the point of impact in the model of interest, (12) can be used to obtain the post-impact angular momentum about the new pivot as a function of the pre-impact state

$$\mathbf{L}^+[k+1] = \mathbf{L}^-[k] - \mathbf{r}_s^-[k] \times m\mathbf{v}_c^-[k]. \quad (13)$$

Similarly, the center of mass relative to the support foot undergoes a discrete change at impact due to support change

$$\mathbf{r}_c^+[k+1] = \mathbf{r}_c^-[k] - \mathbf{r}_s^-[k]. \quad (14)$$

For flat ground walking, (14) and (13) restricted to the forward (\hat{x}, \hat{z}) plane are

$$x_c^+[k+1] = x_c^-[k] - x_s^-[k], \quad (15)$$

$$L_y^+[k+1] = L_y^-[k] + mx_s^-[k]\dot{z}_c^-[k]. \quad (16)$$

Continuous-time controllers for x_s and z_c will be designed to achieve pre-impact values, $x_s^-[k]$ and $\dot{z}_c^-[k]$, corresponding to desired $(x_c^+[k+1], L_y^+[k+1])$ using (15) and (16). A controller for z_s will ensure the swing foot hits the ground according to the desired transfer of forward momentum.

The restrictions of (14) and (13) to the (\hat{y}, \hat{z}) plane are

$$y_c^+[k+1] = y_c^-[k] - y_s^-[k], \quad (17)$$

$$L_x^+[k+1] = L_x^-[k] - my_s^-[k]\dot{z}_c^-[k]. \quad (18)$$

Similar to the horizontal case, continuous-time control of y_s will be designed to stabilize $(y_c^+[k+1], L_x^+[k+1])$.

IV. MECHANICS-BASED CONTROL

This section presents the main contribution of the paper: a controller which stabilizes underactuated robotic walking by operating on the transfer of angular momentum from one leg to the next. The goal will be to construct continuous-time desired trajectories for the robot's swing leg and vertical center of mass – which update continuously as the center of mass and angular momentum evolve – to effect a desired transfer of angular momentum through foot impact and then stabilize to these trajectories via Model Predictive Control.

The final form of the outputs to be constructed is

$$\mathbf{y}(\mathbf{q}, \dot{\mathbf{q}}) = \begin{bmatrix} x_s(\mathbf{q}) \\ y_s(\mathbf{q}) \\ z_s(\mathbf{q}) \\ z_c(\mathbf{q}) \\ \theta_x(\mathbf{q}) \\ \theta_y(\mathbf{q}) \end{bmatrix} - \begin{bmatrix} x_s^d(x_c(\mathbf{q}), \mathbf{k}_x(\mathbf{q}, \dot{\mathbf{q}})) \\ y_s^d(x_c(\mathbf{q}), \mathbf{k}_y(\mathbf{q}, \dot{\mathbf{q}})) \\ z_s^d(x_c(\mathbf{q}), \mathbf{k}_z(\mathbf{q}, \dot{\mathbf{q}})) \\ z_c^d(x_c(\mathbf{q}), \mathbf{k}_c(\mathbf{q}, \dot{\mathbf{q}})) \\ 0 \\ 0 \end{bmatrix}, \quad (19)$$

where $x_s^d(x_c, \mathbf{k}_x)$, $y_s^d(x_c, \mathbf{k}_y)$, and $z_s^d(x_c, \mathbf{k}_z)$ are desired trajectories for the horizontal, lateral, and vertical components of the swing foot, and $z_c^d(x_c, \mathbf{k}_c)$ is a desired trajectory for the vertical center of mass. Coefficients $\mathbf{k}_\square(\mathbf{q}, \dot{\mathbf{q}})$ of the desired trajectories in (19) will be designed to connect initial values for the swing leg and vertical center of mass to desired pre-impact values of these quantities corresponding to a prescribed transfer of angular momentum using the COM and momentum transfer equations (15)–(17). These coefficients are continuously updated based on a future horizon estimate of the pre-impact COM and momentum. The final two outputs encode the auxiliary goal of maintaining an upright torso by driving $\theta_x = q_1 + q_5$ and $\theta_y = q_2 + q_3 + q_4$ to zero.

A. Desired Pre-Impact Kinematics

To stabilize walking, the proposed mechanics-based control approach dictates desired values for the post-impact horizontal $x_c^+[k+1] = x_c^*$ and lateral $y_c^+[k+1] = y_c^*$ components of the center of mass and forward $L_y^+[k+1] = L_y^*$ and lateral $L_x^+[k+1] = L_x^*$ components of the angular momentum. The desired x_c^* and y_c^* are realized through the use of (15) and (17) in the construction of desired trajectories for the swing leg that satisfy the following conditions when the robot reaches pre-impact values x_c^- and y_c^-

$$x_s^d(x_c^-, \mathbf{k}_x) = x_c^- - x_c^*, \quad (20)$$

$$y_s^d(y_c^-, \mathbf{k}_y) = y_c^- - y_c^*, \quad (21)$$

$$z_s^d(x_c^-, \mathbf{k}_z) = 0. \quad (22)$$

Similarly, a desired transfer of forward momentum from a pre-impact value L_y^- to the desired post-impact value L_y^* is realized using (16) via the following condition on the desired trajectory for the vertical center of mass

$$z_c^d(x_c^-, \mathbf{k}_c) = \frac{L_y^* - L_y^-}{m(x_c^- - x_c^*)}. \quad (23)$$

Note that these “boundary conditions” are functions of (x_c^-, y_c^-, L_y^-) , which are unknown in general; however, the following section describes a method of continuously estimating (x_c^-, y_c^-) for a fixed L_y^- using the LIP.

B. Forward Horizon Center of Mass and Momentum

Given the current horizontal center of mass $x_c(\mathbf{q})$ and forward angular momentum, $L_y(\mathbf{q}, \dot{\mathbf{q}})$, the LIP solution described in (8) and (11) can be used to obtain the time T required for the LIP to reach to a future state (x_L^-, L_y^-)

$$T(\mathbf{q}, \dot{\mathbf{q}}) = -\frac{1}{\lambda} \ln \left(\frac{x_L^- \sqrt{gz_0} - L_y^-}{x_c(\mathbf{q}) \sqrt{gz_0} - L_y(\mathbf{q}, \dot{\mathbf{q}})} \right). \quad (24)$$

Substituting (24) for t in the center of mass component of the LIP solution (8) yields

$$x_L^-(\mathbf{q}, \dot{\mathbf{q}}) = \sqrt{\frac{(L_y^-)^2}{gz_0} - \frac{L_y(\mathbf{q}, \dot{\mathbf{q}})^2}{gz_0} + x_c^2(\mathbf{q})}. \quad (25)$$

Thus the horizontal center of mass component of the LIP, x_L^- , corresponding to a specific future value of the angular momentum, L_y^- , can be obtained as a function of the state of the robot on the flow $(\mathbf{q}(t), \dot{\mathbf{q}}(t))$. This motivates the development of a controller which drives the height of the swing foot to zero when the forward momentum $L_y(\mathbf{q}, \dot{\mathbf{q}})$ reaches L_y^- , resulting in an impact occurring at $x_c^- = x_L^-(\mathbf{q}, \dot{\mathbf{q}})$. This provides a moving estimate of the value of the pre-impact center of mass that can be used in (20) and (23) to dynamically produce desired pre-impact values for the horizontal swing leg position and the vertical COM velocity.

Similarly, an estimate of the pre-impact lateral component of the center of mass can be obtained using (24) in the solution to the lateral plane variant of the LIP dynamics

$$y_L^-(\mathbf{q}, \dot{\mathbf{q}}) = \left(\frac{y_c(\mathbf{q})}{2} + \frac{L_x(\mathbf{q}, \dot{\mathbf{q}})}{2\lambda z_0} \right) e^{\lambda T(\mathbf{q}, \dot{\mathbf{q}})} + \left(\frac{y_c(\mathbf{q})}{2} - \frac{L_x(\mathbf{q}, \dot{\mathbf{q}})}{2\lambda z_0} \right) e^{-\lambda T(\mathbf{q}, \dot{\mathbf{q}})}. \quad (26)$$

This provides an estimate $y_L^-(\mathbf{q}, \dot{\mathbf{q}})$ of y_c^- which can be used in conjunction with (21) to dynamically update a desired pre-impact value for the step length in the lateral direction. The following section presents the construction of a desired trajectory for the height of the swing foot which renders (25) and (26) viable moving estimates of the pre-impact COM.

C. Height of the Swing Foot Output Construction

The desired trajectory for the height of the swing foot is designed to keep the foot above the ground until the angular momentum reaches a specified value, L_y^- , at which point the foot is forced to impact the ground. Here, we use a quadratic

$$z_s^d(x_c, \mathbf{k}_z) = k_{z,1}x_c^2 + k_{z,2}x_c + k_{z,3}. \quad (27)$$

The coefficients of (27) are updated at each $(\mathbf{q}, \dot{\mathbf{q}})$ by solving

$$z_s^d(x_c^+, \mathbf{k}_z) = 0, \quad (28)$$

$$z_s^d(x_L^-(\mathbf{q}, \dot{\mathbf{q}}), \mathbf{k}_z) = 0, \quad (29)$$

$$z_s^d(x_c^+ + (x_L^-(\mathbf{q}, \dot{\mathbf{q}}) - x_c^+)/2, \mathbf{k}_z) = z_s^{\max}, \quad (30)$$

where $z_s^{\max} > 0$ is a parameter encoding the maximum height of the foot. Note that these coefficients are dynamically updated in continuous-time; as the pre-impact center of mass estimate $x_L^-(\mathbf{q}, \dot{\mathbf{q}})$ is a function of the current state, the coefficients $\mathbf{k}_z(\mathbf{q}, \dot{\mathbf{q}})$ are likewise a function of the state.

D. Continuous-Time Control

Similar to the height of the swing foot, desired outputs for the forward, x_s^d , and lateral, y_s^d , components of the swing foot and for the height of the center of mass, z_c^d , are constructed to effect the desired transfer of angular momentum described in (20) – (23) using (25) and (26). The resulting output vector (19) has relative degree two [20] along the rigid body dynamics (2)–(3), as the dependence on $\dot{\mathbf{q}}$ appears via the angular momentum and the time-derivative of the angular momentum is independent of the joint torques. The partial feedback linearization control law [20] is given by

$$\mathbf{u}(\mathbf{q}, \dot{\mathbf{q}}) = L_g L_f \mathbf{y}^{-1}(\mathbf{q}, \dot{\mathbf{q}}) (-L_f^2 \mathbf{y}(\mathbf{q}, \dot{\mathbf{q}}) + \mu), \quad (31)$$

where $L_g L_f \mathbf{y}$ and $L_f^2 \mathbf{y}$ are Lie derivatives of the (relative degree two) outputs along the rigid body dynamics and $L_g L_f \mathbf{y}$ is invertible. As described in the following, Model Predictive Control is used to produce a stabilizing μ consistent with torque limits and momentum transfer constraints.

E. Model Predictive Control

Applying partial feedback linearization (31) to the rigid body dynamics (2)–(3) results in a linear control system on the outputs and their derivatives $\eta = (\mathbf{y}, \dot{\mathbf{y}})$; discretization of this control system yields

$$\eta_{k+1} = \underbrace{\begin{bmatrix} 1 & \Delta T \\ 0 & 1 \end{bmatrix}}_{F_{\Delta T}} \eta_k + \underbrace{\begin{bmatrix} 0 \\ \Delta T \end{bmatrix}}_{G_{\Delta T}} \mu_k. \quad (32)$$

for a discrete time-step $\Delta T > 0$. Given an initial condition, $\eta_0(\mathbf{q}, \dot{\mathbf{q}})$, and a sequence of control inputs, $\bar{\mu} = \{\mu_0, \mu_1, \mu_2, \dots, \mu_{k-1}\}$, the value of η after k time-steps, denoted η_k , can be obtained by successively computing (32).

Model Predictive Control [17] is used to obtain the sequence of control inputs $\bar{\mu}^*(\mathbf{q}, \dot{\mathbf{q}})$ that minimizes the future values of the outputs η_k subject to torque and momentum transfer constraints, over a future time-horizon of length $T(\mathbf{q}, \dot{\mathbf{q}})$ seconds, where $T(\mathbf{q}, \dot{\mathbf{q}})$ is the time-to-impact estimate provided by the LIP (24). This horizon results in $N = \text{ceiling}(T(\mathbf{q}, \dot{\mathbf{q}})/\Delta T)$ discrete time-steps. The MPC problem is implemented as a Quadratic Program

$$\begin{aligned} \bar{\mu}^*(\mathbf{q}, \dot{\mathbf{q}}) = \underset{\bar{\mu}}{\text{argmin}} \quad & \eta_N^T P_\varepsilon \eta_N + \sum_{k=0}^{N-1} \eta_k^T P_\varepsilon \eta_k + \mu_k^T R \mu_k \quad (33) \\ \text{s.t.} \quad & A_k \mu_k \leq b_k, \quad k \in \{0, 1, 2, \dots, N\} \\ & A_{eq,k} \mu_k = b_{eq,k}, \quad k \in \{0, 1, 2, \dots, N\}. \end{aligned}$$

Here $P_\varepsilon > 0$, $R > 0$ encode the goal of minimizing future values of the controller outputs. The inequalities A_k and b_k enforce torque constraints $|u_k| \leq u^{max}$ and $A_{eq,k}$ and $b_{eq,k}$ enforce the transfer of momentum described in (23). The constraints can be estimated over a forward horizon using the solution of the angular momentum LIP, together with inverse kinematics on the zero dynamics surface associated with $\mathbf{y}, \dot{\mathbf{y}}$. The simulation in this paper simply uses $A_k = A_0(\mathbf{q})$ and $b_k = b_0(\mathbf{q}, \dot{\mathbf{q}})$ for the torque constraints. The first six entries in $\bar{\mu}^*(\mathbf{q}, \dot{\mathbf{q}})$ are used in the feedback linearization control law (31) to obtain the joint torque-control law $\mathbf{u}(\mathbf{q}, \dot{\mathbf{q}})$.

F. Desired Momentum Transfer for Forward Walking

To achieve forward walking, the desired (x_c^*, L_y^*) and the desired L_y^- are chosen to be in the top (forward walking) quadrant of the phase space of the LIP. Based on the specific output construction, for sufficiently capable continuous-time control, the post-impact forward COM and angular momentum can be driven to values within the forward-walking quadrant of the LIP phase space with arbitrary accuracy.

As mentioned, stabilization of the forward angular momentum is achieved by ensuring that the swing foot impacts the ground when the forward momentum reaches L_y^- . This means, however, that the controller cannot simultaneously achieve an arbitrary post-impact lateral COM and angular momentum. The current lateral control solution is to pick reference values y_c^d and L_x^d and use the angular momentum LIP forward horizon estimate to update the corresponding desired post-impact, lateral component of the center of mass

$$y_c^*(\mathbf{q}, \dot{\mathbf{q}}) = \pm(y_c^d - \rho((L_x^-(\mathbf{q}, \dot{\mathbf{q}}))^2 - (L_x^d)^2)) \quad (34)$$

with $\rho > 0$. The change in sign reflects the alternation of the support foot between the left and right legs. The sequence $y_c^*(\mathbf{q}^-[k], \dot{\mathbf{q}}^-[k])$, $k = \{1, 2, \dots\}$ converges to a fixed point for the simulation and controller configuration considered.

V. SIMULATION RESULTS

The proposed mechanics-based control method is implemented in simulation of the 67.7kg underactuated 3D robot shown in Fig. 1. The equations of motion (2)–(3) are computed using a MATLAB implementation of Spatial Vector Algebra [3] and numerically integrated using MATLAB's `ode45` function. The Mathematica package [15] is used to generate kinematics expressions for the controller.

A. Mechanics-Based Control Setup

The nominal walking height is chosen to be $z_0 = 0.7\text{m}$. Forward walking is encoded through a desired post-impact COM, $x^* = -0.18\text{m}$, $y_c^d = 0.12\text{m}$, and normalized angular momentum values $L_y^* = 0.7$, $L_y^- = 0.75$ and $L_x^d = 0.26$. The desired post-impact lateral center of mass converges to $y_c^* = \pm 0.1\text{m}$ with $\rho = 0.75$. In this example, the desired forward and lateral step lengths, x_s^d and y_s^d , are linear functions of the horizontal center of mass, x_c , the desired height of the swing foot z_s^d is given in (27), and the desired vertical center of mass is z_0 . The MPC is configured with $\varepsilon = 100$ and $R = 0.001I$, $u^{max} = 250 \text{ N}\cdot\text{m}$ and time step $\Delta T = 0.02\text{s}$.

B. Results

The proposed control method under the given parameters drives the system into a periodic orbit, shown in the middle column of Fig. 3. The maximum magnitude of the real part of the eigenvalues of a numerical approximation of the Jacobian of the Poincaré map for the orbit is $0.85 < 1$, which indicates that the orbit, and thus the walking is locally asymptotically stable [8]. The left column shows the corresponding prescribed transfer of angular momentum in the forward and lateral planes, and convergence to these orbits in a simulation starting from perturbed initial conditions. A movie of the simulations can be found online [1].

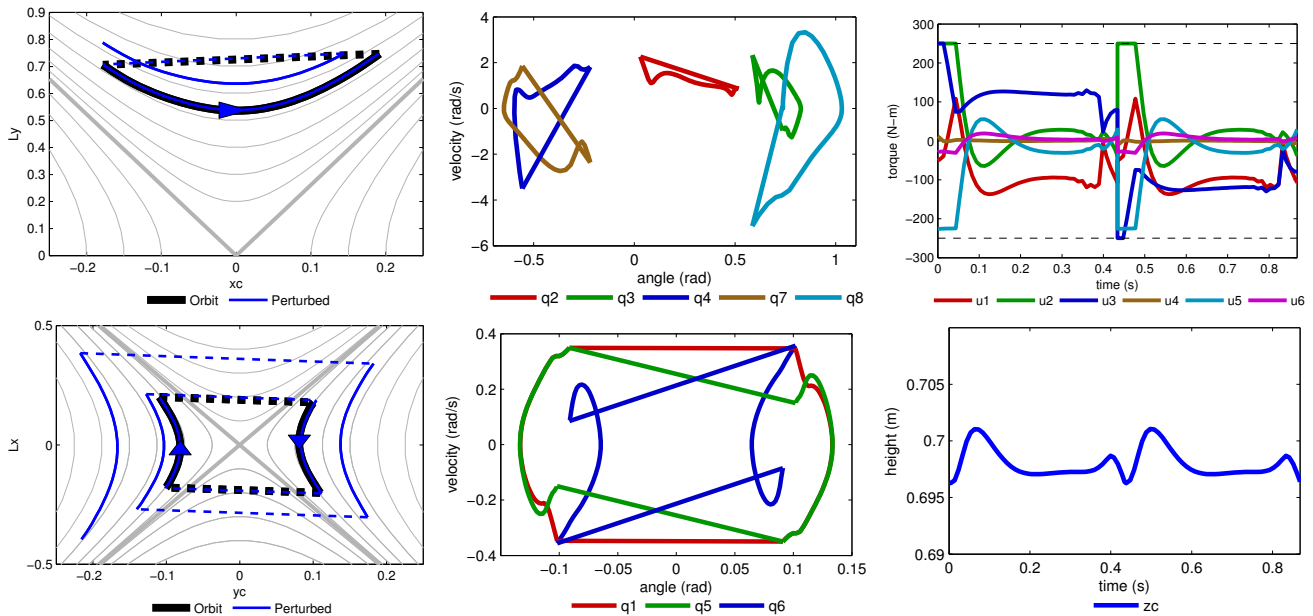


Fig. 3. Simulation results from the application of proposed mechanics-based control approach to underactuated 3D walking. (Left Column) The robot’s post-impact angular momentum and center of mass are driven into regions of a variant of the LIP phase space corresponding to forward walking. Exact expressions for the transfer of angular momentum (15)–(17) allow for the incorporation of discrete effects in the LIP model. (Blue) The flows starting from perturbed initial states converge to the (black) flows along the orbit. (Middle Column) The method results in stable periodic orbits for the (top-middle) pitch angles and (bottom-middle) roll angles. (Top-right) The torques obtained through Model Predictive Control (33) satisfy limits $u^{max} = 250\text{N}\cdot\text{m}$; data is shown for two steps on the orbit (an impact occurs at 0.43 seconds). (Bottom-right) The vertical COM is nominally driven to a constant, however, conditions on the pre-impact velocity (23) are enforced via equality constraints in the MPC-QP (33) to achieve a desired transfer of angular momentum.

VI. CONCLUSION AND FUTURE WORK

This paper presents a novel approach to controlling underactuated walking through regulation of the transfer of angular momentum from one leg to the next. Stability of the resulting walking is verified using numeric Poincaré analysis. Work is currently in progress to show mathematically that application of the proposed method to a hybrid system model of the robot results in stable periodic orbits, and development of an experimental implementation of the method is also underway.

REFERENCES

- [1] <https://youtu.be/kIuuBMWYljM>.
- [2] A. D. Ames. Human-inspired control of bipedal walking robots. *IEEE Transactions on Automatic Control (TAC)*, 2014.
- [3] R. Featherstone. <http://royfeatherstone.org/spatial/v2/index.html>.
- [4] G. Garofalo, C. Ott, and A. Albu-Schaffer. Walking control of fully actuated robots based on the bipedal slip model. In *IEEE International Conference on Robotics and Automation (ICRA)*, 2012.
- [5] B. Griffin and J. Grizzle. Nonholonomic virtual constraints for dynamic walking. In *IEEE Conference on Decision and Control (CDC)*, 2015.
- [6] J. W. Grizzle, C. Chevallereau, and C.-L. Shih. Hzd-based control of a five-link underactuated 3d bipedal robot. In *IEEE Conference on Decision and Control (CDC)*, 2008.
- [7] J. W. Grizzle, C. Chevallereau, R. W. Sinnet, and A. D. Ames. Models, feedback control, and open problems of 3d bipedal robotic walking. *Automatica*, 2014.
- [8] J. W. Grizzle, F. Plestan, and G. Abba. Poincaré’s method for systems with impulse effects: application to mechanical biped locomotion. In *IEEE Conference on Decision and Control (CDC)*, 1999.
- [9] S. Kajita et al. Biped walking pattern generation by using preview control of zero-moment point. In *IEEE International Conference on Robotics and Automation (ICRA)*, 2003.
- [10] S. Kajita and K. Tani. Study of dynamic biped locomotion on rugged terrain-derivation and application of the linear inverted pendulum mode. In *International Conference on Robotics and Automation*, 1991.
- [11] J.-Y. Kim, I.-W. Park, and J.-H. Oh. Walking control algorithm of biped humanoid robot on uneven and inclined floor. *Journal of Intelligent and Robotic Systems*, 2007.
- [12] S. Kuindersma, F. Permenter, and R. Tedrake. An efficiently solvable quadratic program for stabilizing dynamic locomotion. In *IEEE International Conference on Robotics and Automation (ICRA)*, 2014.
- [13] S.-H. Lee and A. Goswami. A momentum-based balance controller for humanoid robots on non-level and non-stationary ground. *Autonomous Robots*, 2012.
- [14] D. Mayne, J. Rawlings, C. Rao, and P. Sokaert. Constrained model predictive control: Stability and optimality. *Automatica*, 2000.
- [15] R. M. Murray, Z. Li, and S. S. Sastry. <http://www.cds.caltech.edu/~murray/mlsWiki/index.php/Software>.
- [16] M. Posa and R. Tedrake. Direct trajectory optimization of rigid body dynamical systems through contact. In *Algorithmic Foundations of Robotics X*, Springer Tracts in Advanced Robotics. 2013.
- [17] M. J. Powell, E. A. Cousineau, and A. D. Ames. Model predictive control of underactuated bipedal robotic walking. In *IEEE International Conference on Robotics and Automation (ICRA)*, 2015.
- [18] J. Pratt, J. Carff, and S. Drakunov. Capture point: A step toward humanoid push recovery. In *IEEE-RAS International Conference on Humanoid Robots*, 2006.
- [19] H. Razavi, X. Da, and A. Bloch. Symmetric virtual constraints for periodic walking of legged robots. In *IEEE Conference on Decision and Control (CDC)*, 2015.
- [20] S. S. Sastry. *Nonlinear Systems: Analysis, Stability and Control*. Springer, 1999.
- [21] B. Stephens and C. Atkeson. Push recovery by stepping for humanoid robots with force controlled joints. In *IEEE-RAS International Conference on Humanoid Robots*, 2010.
- [22] Y. Tassa, N. Mansard, and E. Todorov. Control-limited differential dynamic programming. In *IEEE International Conference on Robotics and Automation (ICRA)*, 2014.
- [23] E. R. Westervelt, J. W. Grizzle, and D. E. Koditschek. Hybrid zero dynamics of planar biped walkers. *IEEE Transactions on Automatic Control (TAC)*, 2003.